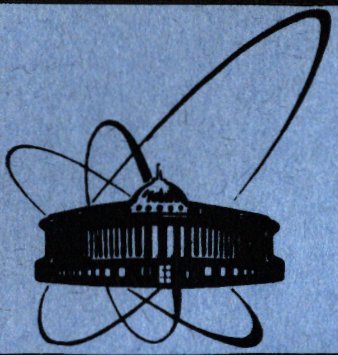

Объединенный
институт
ядерных
исследований
дубна

E7-84-738

P.Mädler

CATAPULT MECHANISM FOR FAST PARTICLE EMISSION IN FISSION AND HEAVY ION REACTIONS

Submitted to "Zeitschrift für Physik A"

1984

1. INTRODUCTION AND MOTIVATION

The emission of light charged particles and neutrons from the neck region during the scission process is a phenomenon known in spontaneous and low-energy neutron-induced fission [1]. Although experimental data on scission neutrons are poor and even partially contradictory[2-7], they more or less agree in about 10% of the prompt fission neutrons to be not consistent with the assumption of evaporation from the fully accelerated fragments, and their average emission energy to be somewhat larger than for the evaporated fraction.

Several theoretical approaches could achieve semiquantitative agreement with experimental scission neutron yields:

i) The emission of such neutrons is related to the non-adiabatic passage from saddle to scission in a characteristic time of a few 10^{-21} s [8] which agrees with the time scale found in more recent hydrodynamical and TDHF studies[9].

ii) Scission itself is considered as a process characterized by a fast increase of the potential barrier between the nascent fragments on a time scale of a few 10^{-22} s [10].

iii) The non-adiabatic return of highly deformed (near scission) fragments to their near-equilibrium deformation enables sufficient transitions of nucleons into the continuum [11], if a return time of $\lesssim 10^{-22}$ s is assumed.

While in i) only the decrease of the neck radius ("necking-in") for a constant depth of the potential was considered, in ii) exclusively the rapid rise of the inner potential barrier has been taken into account. On the other hand, the final stage of the passage of the system from saddle to scission should be the fastest one both with respect to the necking-in degree of freedom and the rise of the inner potential barrier. Moreover, because of largest deformations involved, it should be the beginning and most rapid stage of the transition to a more spherical deformation. Hence, any of the processes modelled in i), ii), and iii) should be most effective in producing neck particles around the scission "point". From this statement it is not surprising that seemingly different aspects of the scission "process" yield similar results.

The time-dependent mean-field theory (TDHF) adapted for the description of large-amplitude nuclear dynamics [12,13] provides a powerful theoretical method for the self-consistent description of the fis-

sion process. The neglect of residual interactions should be more justified in this case than in a description of heavy ion collisions due to the comparably small excitation energies involved in low-energy fission. Despite this, there is only a small number of TDHF studies of fission[9,14-17]. To our knowledge up to now there is no TDHF investigation of non-evaporative particle emission in fission although in this approximation all the aspects discussed above should be contained in a natural way without additional ad hoc assumptions.

In particular, in a recent TDHF study of fission of a slab of charged nuclear matter [15] it was found that the final disintegration of the slab ("snatching") occurs on a time scale which is one order of magnitude shorter than the time required to pass from saddle to scission. "Snatching" was found to appear independently of the choice of the initial conditions used to boost the system beyond the saddle point in order to follow its further time evolution. More realistic TDHF investigations seem to confirm the appearance of "snatching" (compare, e.g., Fig. 6 in [16] or Fig. 7 in [9]) although it is not explicitly stated therein. To see this phenomenon, one must look for sufficiently frequent ($\Delta t < 10^{-22}$ s) plots of the density evolution of the system.

In the present paper we consider the possibility of particle emission connected with the longitudinal (along the scission axis) component of the snatching process. Classically speaking we expect that a nucleon moving with Fermi velocity v_F forwards the inner edge of the self-consistent potential, becomes reflected, and gets velocity $v_F + 2 \cdot v_{cat}$ (v_{cat} denotes a typical velocity of the snatching density tails). If v_{cat} is large enough, the nucleon can escape with an energy

$$\varepsilon = \frac{m}{2}(v_F + 2 \cdot v_{cat})^2 - (\varepsilon_F + B), \qquad (1)$$

ε_F and B being the Fermi energy and the binding energy of the nucleon in the fragment, respectively. For $\varepsilon_F = 37$ MeV and $B = 8$ MeV from (1) one gets a threshold of such a type of particle emission of $v_{cat} = 0.0144\ c$ (c -velocity of light). At $v_{cat} = 0.06\ c$ particles up to $\varepsilon = 30$ MeV can be emitted. For obvious reasons we like to call these particles "catapult particles". Their angular distribution is expected to be peaked around the direction of the scission axis. Moreover, due to refraction at the surface there is some focusing effect for particles coming from the snatching region and crossing the whole fragment.

The appearance of catapult particles is, of course, very much dependent both on sufficiently high "catapult velocities" v_{cat} and a sufficiently strong direct coupling of the collective snatching to the intrinsic Fermi motion to occur. To avoid ad hoc assumptions concerning these points, we investigate the problem in the TDHF approximation.

Since the process of interest should proceed essentially in one dimension (along the scission axis), the use of the effectively one-dimensional slab geometry [12] seems to be a good starting point for qualitative or semi-quantitative purposes. One must, of course, expect quantitative modifications of the results, we are presenting here, if a more realistic geometry will be studied. In particular, we cannot account for the transverse component of the snatching, i.e., the final and fastest stage of the necking-in, and the corresponding particle emission. On the other hand, to get numerically stable results [18] we must use numerical boxes of length $L \approx 200$ fm and a spatial grid-point spacing of $\Delta z = 0.3$ fm. A corresponding realistic TDHF evolution would be very time-consuming so that an extensive variation of initial conditions cannot be envisaged.

In our calculations we use a simplified Skyrme force

$$v(\vec{r}_1, \vec{r}_2) = \left(t_0 + \frac{t_3}{6}\rho\right)\delta(\vec{r}_1 - \vec{r}_2) \qquad (2)$$

with $t_0 = -1090$ MeV·fm^3 and $t_3 = 17288$ MeV·fm^6. The algorithm for solving the one-dimensional TDHF equations is the same as described in [18]. The Coulomb force is not taken into account since a consistent treatment for slab geometry would result in an infinite potential [12]. Consequences of this omission for the fission process of nuclear matter slabs are discussed and separated from the "catapult effect".

In Sect. 2 we investigate the onset of the catapult effect with varying strength of a collective velocity field chosen as initial conditions. In Sect. 3 a particular example is studied in more detail and a connection is made to recent experimental results on high-energy neutron emission in low-energy fission. In Sect. 4 we speculate on the significance of the catapult mechanism for fast particle emission in the exit channel of heavy ion reactions.

2. FISSION OF A SLAB OF NUCLEAR MATTER

We study the response of a slab of thickness $\mathcal{A} = 2.15$ fm^{-2} to a collective initial velocity field which is superimposed to the corresponding static HF-solution. The diameter of this slab corresponds to a realistic nucleus of mass number $A \approx 250$. Its dynamics is determined by the time evolution of 7 single-particle orbitals $\phi_n(z,t)$. At time $t = 0$ each function ϕ_n is written in the form

$$\phi_n(z, t=0) = \bar{\phi}_n(z) \cdot \exp\{i k(z) z\}, \qquad (3)$$

where $\bar{\phi}_n$ means the static HF-solution centred at $z = 0$. The function $k(z)$ representing a coherent (the same for all n) wave-vector distribution in z-direction is chosen to be

$$k(z) = k_0 \cdot \tanh(\alpha z). \qquad (4)$$

It is directed away from the centre $z = 0$ and its absolute value increases as a function of the distance z from the central plane reaching the saturation values $+k_0$ $(z > 0)$, $-k_0$ $(z < 0)$ for

$$|z| \gtrsim 2/\alpha \ . \qquad (5)$$

This type of "collective" excitations was also investigated in [15]. We fix $\alpha = 0.33$ fm^{-1} but vary the strength of the velocity field $v_0 = \hbar k_0/m$ and analyse the corresponding TDHF time evolution with this type of initial excitation. The excitation energy per nucleon brought into the system is given by

$$E^*/A = \frac{m}{2\mathcal{A}} \int_{-\infty}^{+\infty} v^2(z, t=0) \cdot \rho(z, t=0)\, dz \ , \qquad (6)$$

and the velocity field at any instant is

$$v(z,t) = \frac{1}{\rho(z,t)} \frac{\hbar}{m} \sum_{n=1}^{N} a_n \cdot Im\left(\phi_n^* \frac{\partial}{\partial z} \phi_n\right) \qquad (7)$$

with a_n being the (constant) occupation numbers. Due to the Fermi motion in transverse directions $a_n < 1$. The single-particle density is given by

$$\rho(z,t) = \sum_{n=1}^{N} a_n |\phi_n|^2 \ . \qquad (8)$$

The ground state energy per nucleon of the static slab is

$$E/A = \frac{\hbar^2}{2m\mathcal{A}} \left[\sum_{n=1}^{N} a_n \left\{ \int_{-\infty}^{+\infty} \left| \frac{d\bar{\phi}_n}{dz} \right|^2 dz + \frac{\pi}{2} a_n \right\} \right] \qquad (9)$$

$$+ \frac{1}{8\mathcal{A}} \left[3t_0 \int_{-\infty}^{+\infty} \rho^2 dz + \frac{t_3}{2} \int_{-\infty}^{+\infty} \rho^3 dz \right] .$$

Since the Coulomb force is not taken into account, E/A monotonically decreases with increasing $\mathcal{A}$ asymptotically reaching the nuclear matter value of about -16 MeV. In order to fission a slab of $\mathcal{A} = 2.15$ fm^{-2}, say into two equal $\mathcal{A} = 1.075$ fm^{-2} fragments, the excitation energy per nucleon brought in by the velocity field must exceed at least the corresponding mass difference of 0.63 MeV per nucleon.

We first look for the response of the slab to an initial velocity field of strength $v_0 = 0.046$ c which corresponds to $E^*/A = 1.05$ MeV. The time evolution of the density profiles, which results from solving the

corresponding one-dimensional TDHF equations, is illustrated in Fig. 1.

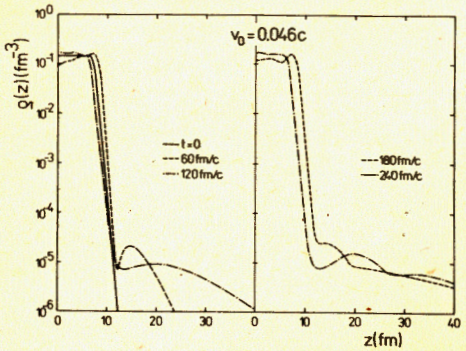

Fig. 1: Time evolution of the density profile $\varrho(z)$ for v_0=0.046 c. Since a symmetric problem is considered, the results are only shown for $z \geq 0$.

We state that no fission occurs. Instead, a large amplitude density oscillation ("breathing mode") is excited. Of course, it does not represent a stationary state, but its main components can seemingly be related to periods around T=120 fm/c corresponding to frequency $\hbar\omega$=10.33 MeV. This value is comparable with a simple classical estimate[12] of the lowest natural frequency of the slab

$$\hbar\omega \approx \frac{\hbar\pi}{L} v_{z.s.} = 11.39 \text{ MeV}. \qquad (10)$$

Here $v_{z.s.}$ = 0.276 c is the speed of zero sound derived for the slab geometry in [12], and L=14.82 fm is the diameter of the slab. Note that the details of the density distribution are by no means periodic in time. Furthermore, it is seen that there is some genuine damping of the slab oscillation due to particle emission. This is indicated by the low-density lumps emerging periodically in front of the slab at each rarefaction phase (t= 60 fm/c, 180 fm/c etc.). The mean energy of the emitted particles is $\bar{\varepsilon}$=3.26 MeV although velocity components corresponding to much higher energies are also present leading to a fast broadening of the low-density tails identified as the emitted fractions of nucleons. The damping of nuclear monopole vibrations in TDHF (an effectively one-dimensional problem too) due to particle emission was investigated in [19].

Next we consider higher v_0 values in order to come closer to fission of the slab. Fig. 2 contains results for the case shown in Fig. 1 as well as for v_0 values of 0.056 c (E^*/A=1.55 MeV), and 0.06 c (E^*/A=1.79 MeV). The time evolution of the density at z =0 as well as the catapult velocity $v_{cat}(t)$ are plotted. The latter is defined as follows: At a given time t it is the maximum value of the actual velocity field $v(z,t)$ in the inner (near z=0) density region of $\varrho(z,t) <$ 0.1 fm^{-3}. This definition gives a measure of the snatching of the inner low-density tails. Except the v_0 =0.046 c case,

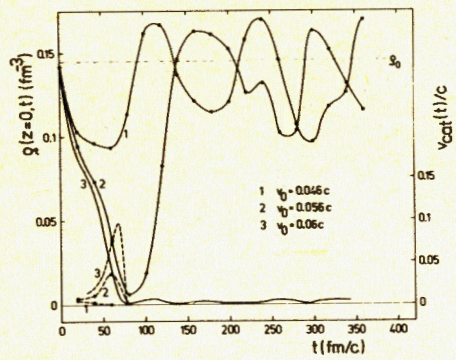

Fig. 2: Time evolution of the density at z =0 (left-hand scale, full lines) for 3 different strengths v_0 of the initial collective velocity field. The "catapult" velocity in units of c (right-hand scale, dashed lines) for each case is also shown (for definition, see text). The full circles are calculated points corresponding to a print frequency of the computer output of Δt= 20 fm/c. The curves are drawn to guide the eye except for the v_0 =0.06c case, where a sufficiently small Δt has allowed to draw smooth lines.

where no snatching occurs, it is unambigous as we shall see below since usually $v(z,t)$ exhibits a sharp peak in z near z=0 during snatching. In the case of the lowest v_0 value $\varrho(z=0,t)$ illustrates the oscillation of the slab as discussed above. Here, the definition of $v_{cat}(t)$ is quite artificial since during the approach of the first rarefaction phase at t= 60 fm/c the velocities in the inner region decrease monotonically. However, already for v_0 = 0.056 c a bend in $\varrho(z=0,t)$ around t =45 fm/c indicating the onset of some snatching correlates with an increase in $v_{cat}(t)$. The catapult velocity reaches a maximum around t = 60 fm/c and falls down to zero at t =80 fm/c, where the two halves of the slab begin to return. After this instant the definition of v_{cat} makes no sense. The first expansion of the slab is clearly of a much larger amplitude than previously while afterwards the density oscillation is more anharmonic and proceeds around a mean value of $\varrho(z=0)$ smaller than the saturation density ϱ_0 =0.145 fm^{-3}.

The v_0 =0.06c calculation obviously represents a transitional case between slab oscillation and fission. Initially the central density falls down to a very small value of 0.002 fm^{-3} at t =76 fm/c. The appearance of snatching is still more pronounced, yielding catapult velocities up to 0.096c at t =68 fm/c. But finally scission does not occur as is seen from the further evolution of $\varrho(z=0)$. For $t >$ 80 fm/c each of the fragments oscillates nearly independently of the other while the distance of their mass centres remains almost constant. In each rarefaction phase of the fragments their densities have a slightly enhanced overlap at z =0 leading to the small maxima in $\varrho(z=0)$ in Fig. 2 at $t >$ 80 fm/c. The density oscillation of the right hand fragment is illustrated in Fig. 3. In analogy with Fig. 1 it is expected to be slightly damped by nucleon emission. The first portion of particles,

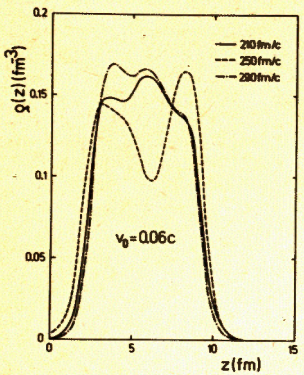

Fig. 3: Density profiles of the right-hand fragment appearing in the case v_0 =0.06c at several instants long after "snatching".

however, is expected to be due to the fast necking-in of $\varrho(z=0)$ ($t \lesssim 40$ fm/c) which is characterized by a substantial stretching of the slab but small velocities in the "neck" region. After finishing the expansion of the system the "catapult" sets in (see v_{cat} in Fig. 2), i.e. we expect a second portion of particles to emerge at a characteristic time $\Delta t = \Delta z/(v_f + v_{cat})$ after the maximum of $v_{cat}(t)$ is reached. Using $v_{cat} = 0.096c$, $v_f = 0.28c$, and the distance from $z=0$ to the point where the catapult particles are expected (forward low-density end of the fragment) to be $\Delta z = 15$ fm we get $\Delta t = 32$ fm/c. Thus they should appear at $t \approx 100$ fm/c. For this instant in Fig. 4 the density profile as well as the velocity field are shown. The arrow in the fragment indicates that after snatching it is in the rarefaction phase connected with an increasing $\varrho(z=0)$. Besides the first portion of emitted particles as expected there is a shoulder in the low-density tail of the fragment. It clearly correlates with a maximum in $v(z)$ at $z=15$ fm. Hence, we may identify this second portion of particles with catapult particles.

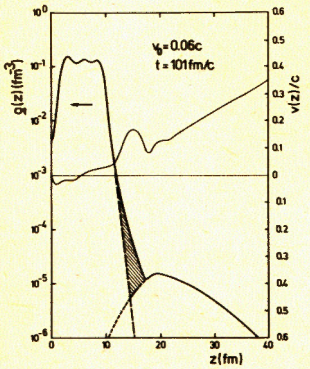

Fig. 4: Density profile (thick line) and velocity field (thin line) for the v_0=0.06c case at t =101 fm/c. The horizontal thin line markes zero velocity (right-hand scale). The long-dashed line extrapolates the exponential fall-off of the fragment density, and the short-dashed line is an extrapolation by hand of the first portion of emitted particles. The hatched region is identified with catapult particles.

We have also investigated still larger v_0 values: 0.064c (E^*/A=2.03 MeV), 0.068c (E^*/A=2.29 MeV), and 0.078c (E^*/A=3.02 MeV). In each of these cases scission occurs and the fragments fly away with certain velocity $v_f(t \to \infty)$. As for 0.06c the necking-in stage is followed by a rapid rise of the velocities in the neck region, i.e., by a pronounced snatching. In Fig. 5 for all investigated examples the maximum of the catapult velocity, the asymptotic velocity of the fragments, and the corresponding total

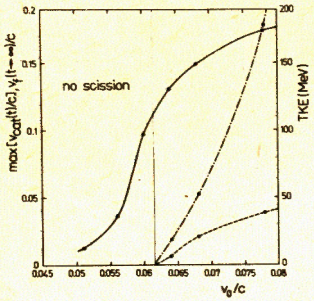

Fig. 5: Maximum catapult velocity (solid line), asymptotic fragment velocity (dashed line), and the total kinetic energy of the corresponding realistic fragments of mass number 126 (dash-dotted line, right-hand scale). Full circles represent calculated points, the lines are drawn to guide the eye. For $v_0 \lesssim 0.05c$ the determination of v_{cat} is ambigous (see text to Fig. 2).

kinetic energy TKE which two fragments of mass number 126 would have in a realistic 3-dimensional case are plotted against the strength of the initial velocity field v_0. We state that although the catapult effect sets in (around $v_0 = 0.051c$, this case was not included in Fig. 2) much below the critical v_0 value at which scission occurs, it rapidly increases in its vicinity. For larger v_0 values this increase is less dramatic. For $v_0 > 0.051c$ it leads to a substantial fraction of catapult particles like it was demonstrated in Fig. 4.

Altogether, the fast snatching of the inner density tails seems to "match" the collective motion of the fissioning slab to the density oscillations of each fragment seperately. It is accompanied by fast particle emission, probably, into directions close to the scission axis in realistic geometry. The fragment oscillations can only decay by particle emission due to the relatively small number of degrees of freedom accessible in the TDHF slab geometry.

3. A PARTICULAR EXAMPLE

We now analyse the case v_0=0.078c in more detail. This is because with respect to both mass numbers and TKE it resembles spontaneous fission of ^{252}Cf. For quantitative comparison with experimental data, however, the excitation energy involved in this case is much too large. This is mainly due to the neglect of the Coulomb force. So, the initial excitation energy has to compensate the mass difference of the initial slab and the final fragments (0.63 MeV/A) as well as the final total kinetic energy (0.71 MeV/A). The remaining fraction (1.68 MeV/A) goes mainly into excitation of the fragments. Despite this we believe that the occurrence of the catapult effect, at least in a qualitative sense, is not artificially caused by the high excitations brought into the system. Our arguments are, first, that a pronounced effect appears already for excitations much smaller than that to get scission, and second, that in similar fission studies of char-

ged nuclear slabs, where the Coulomb force was modelled by a long-range Yukawa-type potential /15/ (in order to avoid an infinite potential), snatching on the same time scale was also obtained, independently of the type of initial conditions (collective velocity field, intrinsic excitations) and already for $E^*/A \approx 0.18$ MeV leading to binary fission.

The time evolution of the density and the velocity field is shown in Fig. 6.

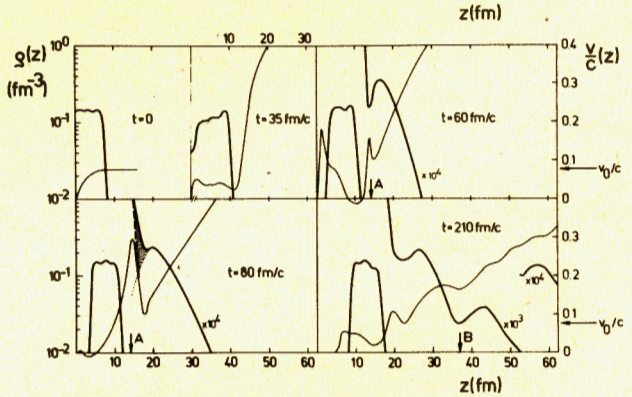

Fig. 6: Time evolution of density (thick lines) and velocity field (thin lines, right-hand scale) for the case $v_0 = 0.078c$. The hatched region is identified with catapult particles similar to the case shown in Fig. 4. The vertical arrows mark the positions of counters A and B for estimating the spectrum (see discussion to Fig. 8).

Due to the unrealistic high initial velocity field the necking-in time characterized by a decrease of the central density, and decreasing (compared to $t = 0$) velocity field, is underestimated by more than one order of magnitude. In the present case it amounts to about 10^{-22}s (30 fm/c). Somewhat later, at $t = 35$ fm/c in the neck region a small peak in the velocity field emerges growing up to a value much larger than v_0 at $t = 60$ fm/c. At this instant the maximum of v_{cat} is reached, which later on quickly decreases similar to the cases shown in Fig. 2. Beginning at $t = 35$ fm/c large velocity components appear in front of the fragment indicating a first portion of particles to be emitted due to the artificially accelerated necking-in process. This portion is clearly seen at $t = 60$ fm/c as a pronounced maximum in the low-density tail correlated with large velocity components. In accordance with the above discussion on the consequences of the omission of the Coulomb force we consider these particles to be spurious (at least highly overestimated). Fortunately, at $t = 60$ fm/c, where the most intensive snatching is observed, we can get an estimate of those necking-in particles. At $t = 80$ fm/c that corresponds to the time after $t = 60$ fm/c a nucleon of velocity $v_0 + 2\max\{v_{cat}(t)\}$ needs to cross the distance from $z = 0$ to $z = 15$ fm a shoulder in the low-density tail of the fragment appears, which can be clearly distinguished from the spurious portion, and which is correlated with a sharp peak in the velocity field in front of the fragment. We identify this fraction of particles with catapult particles.

At a much later instant ($t = 210$ fm/c) both fractions more or less cover each other due to their broad velocity distributions. Moreover, a further peak appears at $z = 27$ fm, which is related to a subsequent decay by particle emission of the density oscillations of the fragment. Since in this oscillations too high energies are involved, they yield substantial amounts of particles, which we also consider to be spurious.

Before estimating the spectrum of the catapult particles we illustrate the transition from the artificially fast necking-in to snatching (catapult). Fig. 7 shows the density distributions for $t = 0$, 35, 60 fm/c in a smaller scale. It is characteristic for the necking-in stage that the system becomes highly stretched and a "neck" (low central density) is formed. The "catapult" fastly, on a time scale of 10^{-22}s, returns the density profile to near-equilibrium shapes of the fragments while the positions of their mass centres remain nearly unchanged. This behaviour is very similar to that illustrated in Fig. 4 of /15/. This is one more indication for the catapult effect to be not artificially caused by the neglect of the Coulomb force.

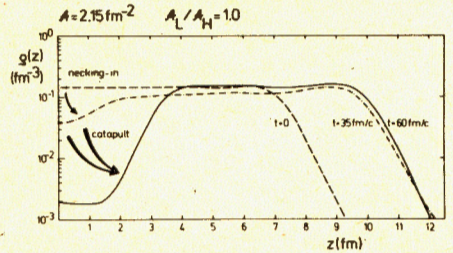

Fig. 7. Time evolution of the density for the $v_0 = 0.078$ c case.

We have kept the evaluation of the energy spectrum of the catapult particles in close analogy to /20/: All the single-particle wave functions have been recorded as functions of time at a fixed "counter" position z_0 outside the fragments and then Fourier analysed with respect to their energy components

$$\tilde{\phi}_n(z_0,\varepsilon) = \frac{1}{2\pi\hbar}\int_0^\tau \phi_n(z_0,t)\cdot\exp\left[\frac{i}{\hbar}\varepsilon t\right]dt \qquad (11)$$

Here τ denotes a time at which the considered signal has sufficiently faded so that the time integration can be considered to go up to infinity. The current density

$$\tilde{j}(z_0,\varepsilon)=\sqrt{2\varepsilon/m}\sum_{n=1}^{N} a_n \left|\tilde{\phi}_n(z_0,\varepsilon)\right|^2 \qquad (12)$$

is proportional to the energy spectrum

$$N(\varepsilon)=\alpha\cdot\tilde{j}(z_0,\varepsilon), \qquad (13)$$

which we have normalized to be comparable with the neutron energy spectrum (per single fission act) of spontaneous fission of ^{252}Cf:

$$\alpha=\frac{2N}{\mathcal{A}}\int_{z_0}^{\infty}\varrho(z,\tau)\,dz\Big/\int_{0}^{\infty}\tilde{j}(z_0,\varepsilon)\,d\varepsilon. \qquad (14)$$

The first integral in (14) counts the number of emitted particles per unit area. The factor 2 is due to the symmetry of the problem with respect to the central plane, and N=154 is the neutron number of ^{252}Cf.

To get a qualitative estimate of the catapult neutron spectrum, we use a counter A at z =14 fm, and a counter B at z=37 fm (compare Fig. 6). Counter A gives us an estimate of the necking-in particle spectrum at τ = 60 fm/c. It is shown in Fig. 8. At τ = 80 fm/c counter A has registered both necking-in and catapult particles.

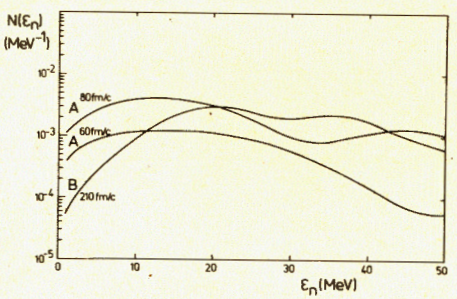

Fig. 8: Neutron spectra for V_0=0.078 c taken at several instants with counters A and B and normalized to be comparable with the spectrum of prompt neutrons from spontaneous fission of ^{252}Cf. For details, see text.

However, there is a substantial contamination from the fragment, which is more pronounced in the latter case since the moving fragment is closer to the counter. This contamination is expected to cover preferentially the lower energy region. To exclude it, we compare with a third spectrum taken at τ=210 fm/c from counter B. As expected, it exhibits a smaller low-energy tail. Unfortunately, this spectrum in turn is contaminated by the high-velocity components of a third fraction of particles (near z =27 fm at t=210 fm/c in Fig. 6), which are also to be excluded as discussed above, but which are hard to estimate.

A further ambiguity is connected with the use of finite τ values at which the signals still have not sufficiently faded (except, may be,

for counter A at τ = 60 fm/c). This is the reason for the unphysical oscillating behaviour of the two other spectra.

Despite these troubles Fig. 8 gives an order-of-magnitude estimate for the catapult neutron spectrum in the considered case: The difference of the two curves above and the lower one yields cataput neutrons in the energy range around 20-30 MeV on a level of 10^{-3} MeV^{-1} per fission act.

In recent measurements of the high-energy end of the prompt neutron spectrum from spontaneous fission of ^{252}Cf /21,22/ and from 14.5 MeV-neutron-induced fission of ^{238}U /21/ fast neutrons in the 20-30 MeV region have been observed on a level of up to 2 orders of magnitude above the values calculated from assuming evaporation from the fully accelerated fragments. The effect is most pronounced for the former case, where in that energy region $N(\varepsilon_n)$ amounts up to nearly 10^{-5} MeV^{-1}. Up to now double-differential cross sections have not yet been measured at these high energies since this would require more complex coincidence measurements connected with still lower intensity. So, the existing experimental data provide a possible evidence for the existence of catapult particles. Other mechanisms which are probably connected with more isotropic or even sidewards peaked angular distributions cannot, however, be excluded at present.

Due to the simple TDHF slab geometry, where most of the degrees of freedom are frozen, the present considerations cannot pretend to be quantitatively relevant. The overestimation of the experimentally observed effect by two orders of magnitude is surely due to the much too high excitations involved in the fission of the slab. Furthermore, although in low-energy fission the fragments are sufficiently cold, for particles of 30 MeV final energy the mean free path in the fragments is about twice as small as their diameter. So, two-body residual interactions would also reduce our predictions in the high-energy tail of the spectrum. Possibly, the catapult particles induce exciton-model type chains to more complex states. The TDHF predictions would then somewhat be damped and broadened in the angular distributions.

4. CATAPULT EFFECT IN SLAB COLLISIONS

While in the slab fission studies the main drawback is an energy balance differing from that in low-energy fission, it is known /12,18/ that with this respect slab collisions come closer to the reality of heavy ion collisions.

We have performed a series of slab collision calculations and always found a more or less pronounced catapult effect. As a typical

example we discuss here the symmetric $\mathcal{A}_1=\mathcal{A}_2=1.075$ fm^{-2}, $(E/A)_{Lab}=$ =12 MeV slab collision illustrated in Fig. 9. The final stage of this collision very much resembles that of the $v_o=0.06$ c case studied in Sect. 2 (compare Figs. 2-5): In the given example we have a transitional behaviour between fusion and deep inelastic collisions since the final fragments oscillate seperately but yet no scission occurs. Surely, the Coulomb force would split the system in the given situation.

At $t=140$ fm/c we first observe a broad low-density peak around $z=27$ fm, which is clearly related to "promptly emitted particles" (PEP) /18/. Furthermore, a sharp peak in the velocity field near $z=0$ indicates a fast snatching of the inner ends of the fragments. At a time needed by a nucleon of velocity v_F+2v_{cat} to appear in front of the fragment, i.e., at $t=180$ fm/c a large peak in the velocity field correlating with a shoulder in the outer low-density tail of the fragment indicates the emission of catapult particles. At this instant the fragment is in its first rarefaction phase (seen both from the density profile and velocity field), so that the central density $\rho(z=0)$ is larger than previously. In anology with the systematics shown in Fig. 5 one can expect an even larger catapult effect if the fragments would fully separate. In the given case the return of density to the central region prevents a further increase of the catapult velocity. The effect vanishes for lower incident energies when the collision yields fusion, i.e., $\rho(z=0)$ does not fall below a critical value where a fast snatching can appear (compare Fig. 2).

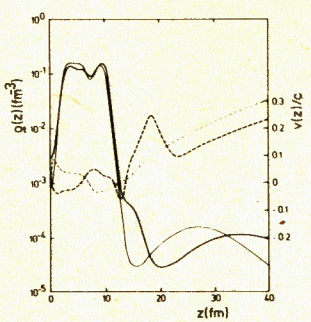

Fig. 9: Density profiles (solid lines) and velocity fields (dashed lines) for a $\mathcal{A}_1=\mathcal{A}_2=1.075$ fm^{-2}, $(E/A)_{Lab}=12$ MeV slab collision at $t=140$ fm/c (thin lines), and $t=180$ fm/c (thick lines).

Based on this result it seems to us that catapult-like particles or particles originating from a multistep-direct chain of more complex exciton states, in principle, could also appear in real heavy ion reactions of the fusion-fission type or even in deep inelastic collisions (the latter being less probable since at too high rebound velocities the fragments separate before being maximally stretched /23,24/). This mechanism would yield non-evaporative particles in the exit channel of a heavy ion reaction, i.e., long after thermal equilibrium of the composite system is established.

Finally, we emphasize that in many realistic TDHF calculations

of heavy ion collisions a more or less pronounced longitudinal snatching behaviour can be deduced from the corresponding plots of the density profiles although, unfortunately, due to the discrete (in time) plots of those results, usually only instants slightly before and after scission are shown. All results which we shall mention below are also contained in /25/ and in the following we quote the corresponding Fig. number in that reference in brackets. The time scales t_s we quote for the snatching are usually upper limits due to the discrete plots.

A very nice example is the $^{16}O+^{16}O$, $E_{Lab}=128$ MeV, $L=25\hbar$ reaction (Fig. 5.4) /26/. Here $t_s\lesssim 50$ fm/c (30 fm/c $\approx 10^{-22}$s). Velocity fields in the reaction plane are also shown indicating fast snatching (although, probably, the maximum of v_{cat} lies between the plots of /26/). For the same system but head-on collisions (Fig. 4.8) /27/ $t_s\approx 10^{-22}$s. At a lower energy, $E_{Lab}=105$ MeV, $L=5\hbar$ (Fig. 5.5) /28/ $t_s\approx 4\cdot 10^{-23}$s for that system. Also for heavy asymmetric systems like $^{84}Kr+^{209}Bi$, $E_{Lab}=600$ MeV, $L=140\hbar$ (Fig. 5.10) /29/ a pronounced snatching seems to occur, $t_s\lesssim 3\cdot 10^{-22}$s. For a very heavy system like $^{238}U+^{238}U$, $E_{Lab}=1785$ MeV, $L=300\hbar$ it proceeds on a somewhat larger time scale: $t_s\lesssim 4\cdot 10^{-22}$s (Fig. 5.15) /30/. There are, however, also a few calculations for heavy systems, which yield a highly stretched neck too but snatching occurs preferentially in the transverse directions and, hence, cannot yield catapult particles. We mention here the $^{136}Xe+^{209}Bi$, $E_{Lab}=1130$ MeV reaction which is illustrated for two values of the initial angular momentum in /31/ (Fig. 6.4). For both $L=0$ and $L=100\hbar$ the shapes of the fragments before and after scission are only slightly changed while in the former case an emerging α-fragment in the neck region is reabsorbed by the target, and in the latter case it appears as a free particle. This transverse "double-snatching" occurs, however, also on a time scale of roughly $1.5\cdot 10^{-22}$s. α-particles from the neck region, which become focused in the transverse directions due to the Coulomb force, have been found in experiment /32/. Preferentially transverse matter flow during scission seems also to be connected with cold fragmentation in low-energy fission /33/.

5. CONCLUSION

We have shown that in one-dimensional TDHF calculations of both fission and collisions of slabs of nuclear matter a fast snatching on a time scale of roughly 10^{-22}s appears to be the final stage of the disintegration of the system, and the beginning of the return of the highly stretched fragments to near-equilibrium shapes of the density. It is connected with the emission of fast particles which we have called "catapult particles".

In the case of fission, induced by an initial collective velocity field, spurious necking-in particles which escape due to the neglect of the Coulomb force and a corresponding far too short saddle-to-scission time have been seperated from the real effect. We have found catapult neutrons on a level, which is about two orders of magnitude higher than in recent experiments on low-energy fission. Since in those experiments only inclusive neutron spectra have been measured, it is not yet clear whether they provide evidence for the catapult effect. In any case, we claim that our fast particle yields in the fission calculations are highly overestimated. This is mainly due to the large excitations involved in these calculations, and to the neglect of the residual interactions which would damp the more or less free matter flow through the fragments. In principle, the latter, as well as pairing correlations could also lead to a stabilization of the shapes of fissioning nuclei and, hence, lower the catapult velocity. This would soften the spectrum of catapult particles.

It is interesting to contrast the possibility of catapult particle emission with that of cold fragmentation in low-energy fission: In the latter case, small excitations of the final fragments are probably due to preferentially transverse matter flow during scission /33/. Hence, the scissioning configuration is characterized by small deformations and comparably small distances of the fragment mass centres leading to a larger Coulomb repulsion and, consequently, large TKE. For the catapult effect to occur one needs highly stretched fragments before scission occurs. Then the longitudinal matter flow (snatching) should be preferred, the fragments scission at larger distances and get small TKE. It is not excluded that with our initial conditions (high v_o) we have somewhat favoured such a situation.

Highly stretched fragments are presumably a case as rare as cold fragmentation. Catapult particles from most probable, intermediate situations are not excluded, but would have smaller energies limited essentially by the deformation energy near the scission point (roughly 10-20 MeV). Shell effects in the yields of catapult particles can be expected on this grounds. After the emission of a high-energy catapult particle the fragment also remains cold and further evaporation of prompt neutrons is prevented.

Our results on slab collisions seem to be less ambigous with respect to the corresponding energies involved in heavy ion collisions. Moreover, it is encouraging that snatching seems to occur also in realistic TDHF evolutions. So, we claim that catapult particles in principle could appear also in the final channel of heavy ion reactions of the fusion-fission type and possibly also in deep inelastic reactions at not too high rebound velocities. Experimentally they, however, would represent only a quite small fraction of the non-evaporative neutrons. They can only be identified in coincidence with at least one heavy fragment. Furthermore, one should have in mind that the directions of that fragment and the catapult neutrons would not fully coincide due to the fact that after the emission of a catapult neutron the fragments continue to interact via the Coulomb force. The corresponding angle difference would give a measure of the degree of stretching of the system during scission.

Acknowledgement:

The author is grateful to R.Reif for valuable hints and discussions, and to V.V.Pashkevitch for a critical reading of the manuscript. Stimulating discussions with D.Seeliger and H.Märten are also gratefully acknowledged.

REFERENCES

1. Vandenbosch R., Huizenga J.R.: Nuclear fission, Academic Press, N.Y., 1973.
2. Bowman H.R. et al. Phys.Rev., 1962, 126, p. 2120.
3. Bowman H.R. et al. Phys.Rev., 1963, 129, p. 2133.
4. Blinov M.V., Kazarinov N.M., Krisyuk I.T. Sov. J. Nucl.Phys., 1972, 16, p. 1155.
5. Piksaikin V.M., Dyatchenko P.P., Kazaeva L.S. Sov. J.Nucl.Phys., 1977, 25, p. 723.
6. Samyatnin Yu.S. et al. Sov. J.Nucl.Phys., 1979, 29, p. 595.
7. Riehs P. Acta Physica Austriaca, 1981, 53, p. 271.
8. Boneh Y., Fraenkel Z. Phys.Rev., 1974, C10, p. 893.
9. Negele J.W. et al. Phys.Rev., 1978, C17, p. 1098.
10. Fuller R.W. Phys.Rev., 1962, 126, p. 684.
11. Rubtchenya V.A. Preprint RI-28, Leningrad, 1974.
12. Bonche P., Koonin S.E., Negele J.W. Phys.Rev., 1976, C13, p. 1226.
13. Negele J.W. Rev.Mod.Phys., 1982, 54, p. 913.
14. Levit S., Negele J.W., Paltiel Z. Phys.Rev., 1980, C22, p. 1979.
15. Dietrich K., Nemeth J. Z.Phys., 1981, A300, p. 183.
16. Okolowicz J., Irvine J.M., Nemeth J. J.Phys., 1983, G9, p. 1385.
17. Nemeth J., Irvine J.M., Okolowicz J. Phys.Lett., 1984, 134B, p. 290.
18. Mädler P. Z.Phys., 1984, A318, p. 87.
19. Stringari S., Vautherin D. Phys.Lett., 1979, 88B, p. 1.
20. Brosa U., Krone W. Phys.Lett., 1981, 105B, p. 22.

21. Märten H., Seeliger D., Stobinski B. In: Proceedings of the Europhysics Topical Conference on Neutron Induced Reactions. Ed. Oblozinsky P., Smolenice, 1982, p. 287.
22. Märten H., Seeliger D. J.Phys., 1984, G10, p. 349.
23. Bertsch G., Mundinger D. Phys.Rev., 1978, C17, p. 1646.
24. Bonasera A., Bertsch G.F., EL-Sayed E.N. Phys.Lett., 1984, 141B, p. 9.
25. Davies K.T.R. et al. Preprint MAP-23, 1982.
26. Cusson R.Y., Maruhn J.A., Meldner H.W. Phys.Rev., 1978, C18, p. 2589.
27. Koonin S.E. Phys.Lett., 1976, 61B, p. 227.
28. Flocard H., Koonin S.E., Weiss M.S. Phys.Rev., 1978, C17, p. 1682.
29. Davies K.T.R., Koonin S.E. Phys.Rev., 1981, C23, p. 2042.
30. Cusson R.Y., Maruhn J.A., Stöcker H. Z.Phys., 1980, A294, p. 257.
31. Dhar A.K. et al. Nucl.Phys., 1981, A364, p. 105.
32. Wilcke W.W. et al. Phys.Rev.Lett., 1983, 51, p. 99.
33. Armbruster P. et al. In: Proceedings 4th International Conference on Nuclei Far from Stability, Helsingør, 1981, CERN 81-09, p. 675.

Received by Publishing Department
on November 16,1984.

Мэдлер П. E7-84-738

Катапультный механизм испускания быстрых частиц
в делении и реакциях с тяжелыми ионами

Процесс деления слоев ядерной материи моделируется в приближении зависящего от времени Хартри-Фока добавлением начального коллективного поля скоростей к статическому самосогласованному решению. В зависимости от его амплитуды либо возбуждаются осцилляции плотности, либо происходит деление. Конечная стадия деления слоя происходит на временной шкале 10^{-22} с и характеризуется острым максимумом в поле скоростей в области "втягивания" внутренних хвостов плотности. Спустя характерное время появляется плечо малой плотности перед фрагментами одновременно с максимумом в поле скоростей. Мы называем эти частицы "катапультными частицами". Недавно полученные экспериментальные данные, возможно, подтверждают существование катапультных нейтронов в низкоэнергетическом делении. Мы также обсуждаем возможность испускания быстрых катапультных частиц в конечном канале реакций с тяжелыми ионами.

Работа выполнена в Лаборатории теоретической физики ОИЯИ.

Препринт Объединенного института ядерных исследований. Дубна 1984

Mädler P. E7-84-738

Catapult Mechanism for Fast Particle Emission
in Fission and Heavy Ion Reactions

The fission process of slabs of nuclear matter is modelled in TDHF approximation by adding an initial collective velocity field to the static self-consistent solution. In dependence on its amplitude either large amplitude density oscillations are excited or fission occurs. The final disintegration of the slab proceeds on a time scale 10^{-22}s and is characterized by a sharp peak in the actual velocity field in the region of the "snatching" inner low density tails. A characteristic time later a low density lump correlated with a peak in the velocity field emerges in front of the fragments. We call these particles "catapult particles". Recent experimental results possibly provide evidence for catapult neutrons in low-energy fission. We also speculate on the significance of the catapult mechanism for fast particle emission in the exit channel of heavy ion reactions.

The investigation has been performed at the Laboratory of Theoretical Physics, JINR.

Preprint of the Joint Institute for Nuclear Research. Dubna 1984